Challenge Journal of Concrete Research Letters

**Research Article**

# Calcium aluminate cement based high early strength engineered cementitious composites with recycled artificial flaws

Ahmed Latif Kadhim [a], Süleyman Bahadır Keskin [a,*]

[a] *Department of Civil Engineering, Muğla Sıtkı Koçman University, 48000 Muğla, Türkiye*

## ABSTRACT

Engineered Cementitious Composites (ECC) is an ideal repair material due to its high durability and ductility. However, providing ECC with high early strength is challenging since strength and ductility, which are key to crack-free repair, are also interdependent. Thus, it is necessary to use artificial flaws in order to keep the ductility at reasonable levels while increasing the strength. This study uses calcium aluminate cement, a non-portland cement, as the primary binder to attain the early strength in the production of high early strength ECC for the first time. Besides, expanded glass and crumb rubber, both made by recycling waste materials, were included as artificial flaws to enhance ductility. The performance of designed high early strength ECC was assessed through mechanical, abrasion, shrinkage and non-destructive tests and compared with high early strength portland cement based ECC. It is revealed that a minimum compressive strength of 28.9 MPa and flexural strength of 7.1 MPa could be attained even at the age of as early as 6 hours after casting. Nevertheless, deformation capacities were significantly improved after 24 hours following the casting by the use of both artificial flaws. In addition, acceptable drying shrinkage and abrasion resistance values were obtained.

## ARTICLE INFO

*Article history:*
Received 12 June 2024
Revised 10 July 2024
Accepted 1 August 2024

*Keywords:*
Engineered cementitious composites
Expanded glass
Crumb rubber
Calcium aluminate cement
White portland cement



## 1. Introduction

Concrete structures are susceptible to deterioration due to low durability emerging from insufficient tensile strength and ductility (Frangopol and Furuta 2001). Whether the major cause of damage is an internal or an environmental condition, mechanical loading, or even their combination (FHWA 1998; Yunovich and Thompson 2003) they influence the serviceability of structures and threaten human safety. Repair, retrofit, and maintenance of existing structures emerge as an immediate necessity as failure may occur catastrophically if the structures are left in their current condition. While many well-established techniques have been suggested for retrofitting until now, significant engineering and economic challenges remain (Tarhan and Uysal 2024). Studies addressing this issue show that billions of dollars are spent yearly in the USA (Yunovich and Thompson 2003; Emmons and Sordyl 2006) and Asia, and maintenance and repair expenses account for roughly half of the building budget in the UK (Raupach 2006). The total estimated cost of rehabilitation of infrastructures is enormous, reaching multiple trillion dollars in the US and Asia separately and not less than tens of billion dollars on annual basis with repair costs exceeding the cost of new constructions in Europe and Far Eastern countries (Woudhuysen and Abley 2004; Şahmaran and Li 2010).

Although the need for repair and maintenance is inevitable, the repair materials most of the time are not sufficient to meet this need. It is reported that half of the repair fails prematurely while three-quarters of the failure is due to a deficiency in the durability of the repair material (Whiting and Nagi 1994; Emmons 1996; Wang and Li 2006; Li and Li 2011a; Yildirim et al. 2015). Thus, there is a significant demand for durable repair materials to address the need for long-lasting repairs and decrease the associated economic burden. Engineered Ce-

* *Corresponding author.* Tel.: +90-252-211-5469 ; E-mail address: sbkeskin@mu.edu.tr (S. B. Keskin)
ISSN: 2548-0928 / DOI: https://doi.org/10.20528/cjcrl.2024.04.002

mentitious Composites (ECC), which offers high ductility and durability, emerges as one prominent example of materials that can solve this problem. ECC is a type of high-performance cementitious composite with fiber reinforcement that is highlighted with characteristics of high ductility with a strain hardening behavior under uniaxially applied tensile stresses (Yokota et al. 2008). Although the ingredients of ECC are not remarkably different from ordinary fiber-reinforced concrete, they should have the properties designated by considering the matrix, fiber, and matrix-fiber interface properties imposed by the micromechanical-based design theory (Li 1994; 1997). ECC can reach a strain capacity ranging from 3 to 5% under tension by using 2% of polyvinyl alcohol (PVA) fibers while providing compressive strengths between 30 to 100 MPa (Li et al. 2001; Li 2003). Having a tensile strain capacity reaching up to 500 times that of ordinary concrete, ECC can also perform similarly under flexural loading (Li et al. 1994; Li 1997; Li and Kanda 1998). ECC is demonstrated to be an extremely durable material even in the cracked state (Sahmaran and Li 2009) due to the limited crack width as it performs a steady-state crack propagation rather than a Griffith-type cracking observed in the brittle cementitious composites. This kind of ductile behavior observed in ECC is only possible when the cracking strength of the matrix is lower than the fiber bridging strength and provided that the matrix fracture toughness is low enough (Li 2003; Yang and Li 2007).

Although ideal repair materials should gain adequate strength at the specified age, no formal criterion for minimum compressive strength is defined in the current standards. However, based on the infrastructural requirements, minimum values of flexural or compressive strengths at specific early ages may be recommended by the authorities (Parker and Lee Shoemaker 1991; Kurtz et al. 1997; Wilson et al. 1999). The chemical and physical deterioration of concrete over time is influenced by the presence and movement of harmful substances within the concrete, combined with the cumulative impact of applied loads. The degradation of the structure must be evaluated to determine the most suitable repair approach (Preetha et al. 2023). In some cases, the repair work should be completed and infrastructural facilities need to be put back into service in a short time which is more notable in the case of pavements as the repair process should take 6 to 8 hours during the evening time in order to be able to reopen the road to the traffic in the following morning (Wang and Li 2006; Li and Li 2011b; Şahmaran et al. 2015).

Therefore, strength gaining of the repair materials should be very rapid during the early age. However, such an increase following a rapid reaction may cause a remarkable shrinkage and result in cracking. Conventional ECC is a preferential long-lasting repair material (Lim and Li 1997; Li 2004) as a result of very low cracking potential owing to the high deformation capacity even though it may exhibit considerable autogenous shrinkage due to the high amount of binders and very low w/c ratio used (Keskin et al. 2014). Nonetheless, cracks may also initiate due to various environmental and service conditions (Whiting and Nagi 1994). Accordingly, for sustainable repair and maintenance, the repair material should be resistant to induced tensile stresses and thus should possess sufficient tensile or flexural characteristics to eliminate the mentioned drawbacks. On the other hand, the design of a high early strength ECC (HES-ECC) requires special attention as the early strength rise in ECC accompanies the increase in the fracture toughness which in turn results in insufficient ductility. To overcome this, several studies were undertaken which used a rapid hardening binder for high early strength together with an artificial flaw to decrease the fracture toughness and therefore maintain adequate ductility. One of the studies used rapid hardening Type I and Type III portland cement along with polypropylene and polystyrene particles as artificial flaws and revealed the positive effect of the artificial flaws on ductility (Wang and Li 2006). Polystyrene beads with Type III cement were also used in another study to produce HES-ECC for repair purposes (Li and Li 2011b). Ground slag and CEM I 52.5 R type (high early strength) portland cement were used as binders in a study where the 50% by volume of the quartz sand used as aggregate in ECC was replaced with saturated lightweight perlite aggregate to produce HES-ECC (Yildirim et al. 2015). Significant reductions in the matrix fracture toughness and improvements in tensile strain capacity were observed with the lightweight aggregate replacement (Şahmaran et al. 2015). In a study, the cracking potential of conventional ECC was reduced through lowering the elastic modulus by the use of micronized recycled rubber as a replacement for iron ore tailings aggregates. Matrix fracture toughness was reduced with the increase in the replacement amount and improved the strain capacity accordingly (Huang et al. 2013).

In this study, two different types of cement namely high early strength white portland cement (WPC) CEM I 52.5 R and calcium aluminate cement were used as binders. Calcium aluminate cement (CAC) is a type of non-portland cement with prominent properties of very high early strength and high durability. Hydration characteristics are completely different from ordinary portland cement (OPC) and due to specific compound composition, binary and ternary systems can be formed by using CAC for particular purposes due to the interactions between the compounds of the CAC and other binders. Previously Kim et al. (Kim et al. 2003) used, as an admixture, 5% CAC of the total cementitious material to modify the viscosity of ECC to be used for shotcreting. Similarly, CAC was also used in 3D printable ECC design as an admixture at low amounts, to provide early flowability and manipulate the rate of hardening (Soltan and Li 2018). It is known that in such binary systems created by combining portland cement with a low amount of calcium aluminate cement, the stiffening is quite rapid due to the immediate ettringite formation. However, in this study as the aim is not set to achieve an immediate stiffening but rather to reach a sufficient early strength at 6 hours, calcium aluminate cement is used as a major binder, an alternative to high early strength portland cement, due to its early strength attributes associated with CA hydration which results in a slower setting but rapid hardening as a result of $CAH_{10}$ formation (Kırca 2006). Literature studies regarding the design of high early strength ECC have not reported the use of CAC as a major binder yet.

Although high early strength types of cement similar to the white portland cement employed in this study have previously been used to produce HES-ECC in the literature, this study stands alone as it evaluates the use of CAC and compares it with a portland-type cement in several aspects including durability and mechanical properties.

Nevertheless, in order to maintain ductility, expanded glass beads and crumb rubber particles were used with both of the binders. Several researchers have focused on the use of crumb rubber in ECC production in order to prevent spalling due to the vapor pressure in the case of a fire in the literature. Crumb rubber was also found to be effective in enhancing the elasticity of normal strength ECC while additional precautions such as using nanomaterials are required to compensate for the reduced strength due to rubber usage (Al-Fakih et al. 2021). A lower elastic modulus is also beneficial in the case of ECC usage for repair purposes as it can decrease the cracking potential (Huang et al. 2013). For this reason, crumb rubber was also incorporated in this study as it can improve ductility and limit cracking potential simultaneously. Spherical expanded glass beads were also utilized as an alternative flaw in this study. Although glass has been used to produce lightweight ECC in previous studies (Li 2012), for the first time thermally expanded glass, made out of recycled glass is used for high early strength purposes due to its distinctive characteristics compared to the rubber particles. Compared to previous studies, this study stands out in terms of providing early strength and ductility in many ways, mainly by using calcium aluminate cement as a major binder. In previous studies, CAC was used as an admixture due to its interaction with portland cement. Although waste rubber has been used in the production of ECC due to its elastic properties and expanded glass due to its low density, these two materials have been considered for the first time as an artificial flaw for high early strength. In addition, artificial flaws were also used with high early strength white portland cement to produce HES-ECC with similar early strength to CAC-based HES-ECC and mechanical, non-destructive, and shrinkage properties were compared. In brief, this study aims to evaluate the potential for producing high early-strength ECC by combining the high early-strength properties of calcium aluminate cement with the deformation capacity provided by the recycled artificial flaws.

## 2. Materials and Method

### *2.1. Materials and mixture proportions*

In the production of HES-ECC mixtures, two types of cement: white portland cement and calcium aluminate cement were used. White portland cement (CEM I 52.5 R type) was selected due to its high early strength. Calcium aluminate cement conforming to EN 14647 (EN 14647 2007) standard on the other hand is a commonly used binder for repair mortars and is chosen as it can reach its ultimate strength within a day. In addition, as conventional ECC mixtures contain a high amount of fly ash in composition per micromechanical-based design theory, it was decided to use as much fly ash as possible, provided that the mixtures reach sufficient early strength. However, this could only be possible in the case of CAC-containing mixtures. Class C fly ash obtained from the Yatağan thermal power plant, was used as a secondary binder. Detailed chemical analysis and physical properties of the binding materials are provided in Table 1.

**Table 1.** Chemical compositions and physical properties of the binding materials.

| Chemical Analysis | CAC (%) | WPC (%) | Fly Ash (%) |
|---|---|---|---|
| SiO2 | 3.76 | 21.6 | 50.04 |
| $Al_2O_3$ | 39.48 | 4.05 | 22.85 |
| $Fe_2O_3$ | 17.23 | 0.26 | 8.02 |
| CaO | 36.91 | 65.7 | 11.21 |
| MgO | 0.45 | 1.3 | 2.23 |
| $SO_3$ | 0.01 | 3.3 | 0.78 |
| $Na_2O$ | 0.12 | 0.03 | 0.27 |
| $K_2O$ | 0.14 | 0.35 | 2.50 |
| Physical Properties | | | |
| Specific Gravity | 3.27 | 3.06 | 2.28 |
| Blaine fineness ($cm^2/g$) | 3150 | 4600 | 2850 |

Two types of artificial flaws were used in the production of HES-ECCs, crumb rubber from scrap tires and spherical granules of expanded glass from recycling, to compensate for the matrix fracture toughness, which would otherwise increase due to the use of high-strength binders. Both artificial flaws were included in the mixtures at 5% of the total volume. While the specific gravity of the crumb rubber was 1.15, its particle sizes were in the range of 0.42 to 4.75 mm with the majority larger than 2.36 mm. The specific gravity of the expanded glass granules was 0.4 and the particle sizes ranged from 2 to 4 mm. A picture of both artificial flaws is provided in Fig. 1.

**Fig. 1.** Artificial flaws used.

Although several types of fibers have been used to produce ECC in the literature, PVA fibers stand out due to exceptional mechanical performance and economic advantages. For this reason, 2% of PVA fibers by volume, as adopted by previous studies following the micromechanical-based design theory, were used in all mixtures throughout the experimental study. The PVA fibers have a specific gravity of 1.3, a length of 8 mm, a diameter of 39 µm, and a tensile strength of 1600 MPa, as provided by the manufacturer.

Polycarboxylate ether-based high range water reducing admixture (HRWRA) corresponding to Type F according to ASTM C494 standard (2013), with a specific gravity of 1.1 and 40% solid content was used to enhance the workability of the mixtures. In addition, in the production of HES-ECC, those include white portland cement as the main binder an accelerating admixture (AA) corresponding to Type C according to ASTM C494 standard (2013) was used to reach the target strength. For the mixtures containing calcium aluminate cement, lithium carbonate (LC) salt was used as an accelerator.

### *2.2. Test specimen preparation and testing*

To decide on the mixture proportions given in Table 2, a preliminary study was carried out in which the consistencies of the mixtures along with the compressive and flexural strengths were evaluated. Although fly ash is a latent hydraulic material, in the first group of mixtures where the calcium aluminate cement is the main binder, sufficient strength values could be reached even without eliminating the use of fly ash, although the amount used is lower than the conventional ECC. Nevertheless, the pozzolanic reaction is very limited due to the lack of portlandite as a product of CAC hydration (Ideker et al. 2019), fly ash may help decrease the fractural toughness and contribute to flexural performance. In the second group of mixtures that contain white portland cement, fly ash replacement resulted in strength values lower than expected. Hence, the second group was produced by using WPC alone as a binder. The proportions of all mixtures used in the study are provided in Table 2.

**Table 2.** HES-ECC mixture proportions.

| Ingredient (kg/m$^3$) | C-CAC | EG-CAC | R-CAC | C-WPC | EG-WPC | R-WPC |
|---|---|---|---|---|---|---|
| Total water | 344 | 327 | 327 | 360 | 342 | 342 |
| CAC | 812 | 770 | 770 | - | - | - |
| WPC | - | - | - | 1333 | 1265 | 1265 |
| Fly ash | 464 | 440 | 440 | - | - | - |
| Quartz sand | 459 | 436 | 436 | 480 | 455 | 455 |
| Expanded glass | - | 20 | - | - | 20 | - |
| Crumb rubber | - | - | 58 | - | - | 58 |
| PVA fiber | 26 | 26 | 26 | 26 | 26 | 26 |
| HRWRA | 12.75 | 12.10 | 12.10 | 13.33 | 12.65 | 12.65 |
| LC | 0.162 | 0.154 | 0.154 | - | - | - |
| AA | - | - | - | 13.33 | 12.65 | 12.65 |
| Water/Binder | 0.27 | 0.27 | 0.27 | 0.27 | 0.27 | 0.27 |
| Sand/Binder | 0.36 | 0.36 | 0.36 | 0.36 | 0.36 | 0.36 |
| Fly ash/Cement | 0.57 | 0.57 | 0.57 | - | - | - |
| LC/CAC (%) | 0.02 | 0.02 | 0.02 | - | - | - |
| AA/Binder (%) | - | - | - | 1 | 1 | 1 |

A 20-liter capacity planetary-type mixer was used to produce six different HES-ECC mixtures. All solid materials, including binders, silica sand, and lithium carbonate (in the case of CAC) were introduced into the mixer. Water was added slowly while mixing the solid materials until the homogenization of the mixture is reached. HRWRA and PVA fibers were introduced to the mixture subsequently following the water and artificial flaws. Finally accelerating admixture was included in the case of the second group of mixtures.

Immediately after mixing, flow diameters were measured using a 60 mm high flow cone with 70 and 100 mm top and bottom diameters, respectively. The cone was placed on a glass plate and mutually perpendicular diameters were measured. Flow values were also measured for fresh HES-ECCs before fiber was added, a flow diameter of 36±1 cm was aimed before the introduction of PVA fibers for all mixtures used in the study. Although it was possible to achieve higher flow values with the use of additional HRWRA, this was avoided to prevent excessive bleeding.

### 2.2.1. Mechanical testing

The mechanical performances of the produced HES-ECC specimens were evaluated through compressive and flexural tests conducted at 6 hours, 24 hours, 7 days, and 28 days after casting. The specimens, which were left to cure autogenously in closed molds for the first six hours, were taken out of the molds and subjected to testing. Until testing, the specimens to be used in the consecutive test ages were cured in plastic bags at 95±5% RH and 23±2 Cº. Compressive strengths were determined on cubic specimens with dimensions of 50×50×50 mm following the ASTM C109 standard (2020). Flexural strength and midspan deflection capacities were determined under a four-point bending test setup on prismatic specimens with dimensions of 360×75×50 mm located symmetrically on two supports and two loading rollers 304 and 101 mm apart, respectively. The test was carried out at a loading rate of 0.005 mm/sec by using a deformation-controlled electromechanical universal testing machine. Three specimens were used for all mechanical tests at each test age and the results obtained were averaged.

High early-strength materials are typically susceptible to abrasion even at very early ages as they are designed to restore existing infrastructures so that they can be put into service in a short time. Abrasion could take place as a result of several influences and is dependent on factors such as strength, curing, and aggregates used. Abrasion resistance is of greater importance in this particular case, as weak materials such as artificial imperfections can easily increase wear. Thus, abrasion resistances of the developed HES-ECC mixtures were also investigated based on ASTM C944 (2007) standard along with the other mechanical tests. At each test age, one side of cubic specimens with a side length of 150 mm was abraded with rotary cutters under a load of 197 N for 6 minutes, and the depths of wear were measured.

### 2.2.2. Drying shrinkage measurements

As repair materials should be free of cracks, to foresee the potential risks related to cracking and evaluate the effect of the artificial flaws, drying shrinkages of the developed HES-ECC mixtures were investigated. For this purpose, three 25×25×285 mm bar specimens with gauge studs located at both ends were prepared for each mixture, and length changes of the bars were measured by ASTM C596-18 (2007) standards. The first comparator readings were taken after the initial curing for 6 hours, then the specimens were subjected to drying at 23±2 °C and 50±5% RH until the end of 90 days during which the intermediate readings were taken at 24 hours, 7 days, 14 days, 21 days, 28 days, 56 days. Distribution of the artificial flaws through the cross section of the HES-ECC bars are shown in Fig. 2.

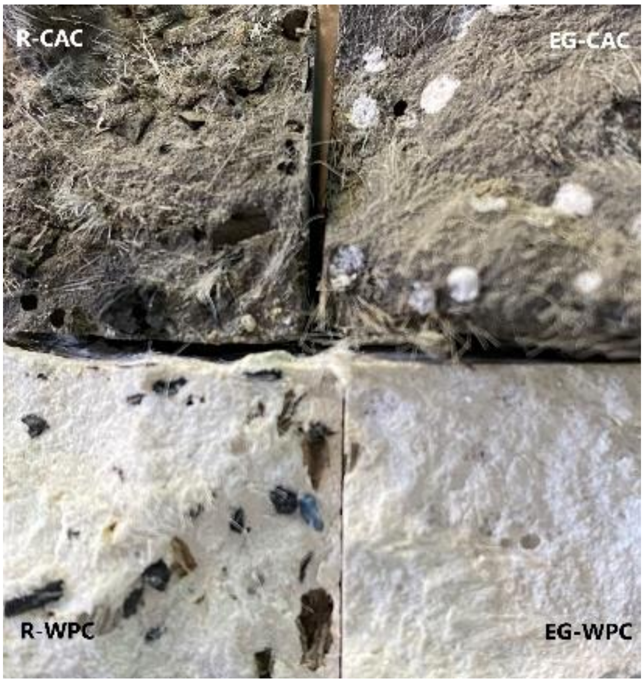


**Fig. 2.** Distribution of artificial flaws.

### 2.2.3. Non-destructive testing

Besides the abovementioned tests, non-destructive tests were also conducted on the mixtures to assess the influence of the artificial flaws. Non-destructive methods of ultrasonic pulse velocity (UPV), resonance frequency (RF), and electrical impedance (EI) were applied at the ages of 6 hours, 24 hours, 7 days, and 28 days on beam specimens with the same dimensions employed in bending tests. UPV tests were conducted using an indirect transmission method with transducers capable of generating and receiving 54 kHz ultrasonic waves, located 20 cm apart. RF tests were conducted by measuring the fundamental longitudinal and transverse frequencies of concrete prisms and corresponding dynamic Young's moduli were calculated in accordance with the ASTM C215 standard (1998). The longitudinal frequencies were determined by locating the accelerometer at the center of one end of the specimen and applying the driving force at the opposite end to excite a vibration through the longitudinal axis of the specimen while the transversal frequencies were measured by locating the accelerometer close to the end of one surface and applying the driving force to the middle point of the same surface to excite a transversal vibration. Although the EI is a very fast and practical test, it allows for evaluating the durability and permeability of concrete. During the test, beam specimens were located vertically between the parallel plate electrodes while wet sponges were put between the specimens and the electrodes to provide conductivity. Despite the EI test being a simple yet effective way to evaluate durability, it is based on complicated essence. Due to the polarization effect encountered under direct current, alternating current is used in the test, and impedance is measured which requires to be converted to resistivity later on. Measurements were taken by using alternating current at fixed frequencies of 1 kHz which yields the lowest phase angle of 0$^o$ and gives a resistance equal to the impedance. Then, the resistivity of the specimen is calculated by Eq. (1):

$$\rho = \frac{A}{L} z \quad (1)$$

where $\rho$, $A$, $L$, and $Z$ are respectively the resistivity, cross-sectional area, length, and impedance of the specimen (Spragg et al. 2013).

## 3. Results and Discussion

### *3.1. Fresh properties*

Flow diameters measured before and after the fiber addition are both provided in Table 3. A matrix slump value of around 36 cm could be achieved by the use of chemical admixtures. In general, although both types of cement have similar matrix consistency, the flow values after the fiber addition were significantly higher for the mixture with WPC. The addition of artificial flaws seems to improve the consistency, as a slightly lower amount of admixtures was needed to achieve the same flow value. In addition, for both types of cement, the flow values of fresh ECC were to some extent higher for the mixtures with flaws.

**Table 3**. Flow diameters of HES-ECC mixtures with and without fibers.

| Mix ID | Matrix (cm) | ECC (cm) |
|---|---|---|
| C-CAC | 35.5 | 11.0 |
| EG-CAC | 36.0 | 13.0 |
| R-CAC | 36.0 | 14.0 |
| C-WPC | 36.0 | 16.0 |
| EG-WPC | 36.5 | 18.0 |
| R-WPC | 36.0 | 17.0 |

### *3.2. Mechanical performance*

Table 4 presents the average compressive strengths for the HES-ECC mixtures at each testing age. For a high early strength repair material, in most cases, the compressive strength at the age of 6 hours is considered as a benchmark. Although the compressive strength to be reached at 6 hours varies according to different sources, in this study a minimum compressive strength of 28.9 MPa even in the presence of flaws could be reached. The control set of CAC mixtures achieved the highest compressive strength at 6 hours due to the rapid formation of calcium alumina hydrates with the help of lithium carbonate salt. The inclusion of the flaws for CAC mixtures resulted in a notable decrease in strength compared to the mixtures with WPC at very early ages. However, as the rate of strength development diminished after 7 days, the gap between the strength of the mixtures was significantly reduced. The control mixture containing WPC, on the other hand, had a lower compressive strength than CAC at 6 hours but eventually surpassed it at later ages. With the use of artificial flaws, a greater reduction in strength was observed in CAC mixtures at early ages, while the decrease in strength of WPC mixtures was more at later ages.

**Table 4**. Compressive strength of HES-ECC mixtures.

| Mix ID | Compressive Strength (MPa) | | | |
|---|---|---|---|---|
| | 6 hours | 24 hours | 7 days | 28 days |
| C-CAC | 35.2 | 51.6 | 57.1 | 60.6 |
| EG-CAC | 29.0 | 41.2 | 48.1 | 56.5 |
| R-CAC | 28.9 | 40.2 | 44.9 | 51.8 |
| C-WPC | 31.6 | 52.0 | 68.9 | 87.9 |
| EG-WPC | 30.2 | 45.7 | 58.6 | 73.3 |
| R-WPC | 29.3 | 41.1 | 56.6 | 66.9 |

The flexural strength and mid-span deflection values of the mixtures as the average of three beam specimens are given in Table 5. Flexural strengths clearly show a similar trend to compressive strengths although the flexural strength development with time was limited since flexural strength is dependent on more complex material characteristics (Qian and Li 2007). Artificial flaws in HES-ECC resulted in a reduction in flexural strength test results across all ages. However, the descending trend was more obvious in the case of incorporating the rubber particles as artificial flaws in R-CAC and R-WPC mixtures which is also evident from the compressive strength results. Even in this case, flexural strength values are well above the values accepted as the minimum flexural strength of concretes to be used for repair purposes by different sources.

**Table 5.** Flexural behavior of HES-ECC mixtures.

| Mix ID | Flexural strength (MPa) | | | | Mid-span beam deflection (mm) | | | |
|---|---|---|---|---|---|---|---|---|
| | 6 h | 24 h | 7 d | 28 d | 6 h | 24 h | 7 d | 28 d |
| C-CAC | 9.5 | 9.8 | 10.9 | 12.0 | 6.5 | 4.2 | 3.0 | 3.0 |
| EG-CAC | 7.8 | 9.6 | 10.7 | 11.3 | 4.4 | 5.5 | 3.3 | 3.8 |
| R-CAC | 7.3 | 8.6 | 10.1 | 10.8 | 4.9 | 5.0 | 3.8 | 3.5 |
| C-WPC | 7.6 | 11.9 | 13.4 | 13.9 | 6.8 | 2.8 | 2.1 | 1.9 |
| EG-WPC | 7.6 | 11.5 | 12.9 | 13.3 | 6.4 | 3.7 | 3.4 | 3.9 |
| R-WPC | 7.1 | 10.3 | 12.2 | 12.4 | 7.7 | 4.3 | 3.2 | 3.1 |

Deformation capacities of the control mixtures began to show a downward trend from the 6th hour due to improved matrix toughness which agrees with Wang and Li (2006) and can be attributed to the development of the interfacial bond between the fibers and the matrix. Despite the decline in deformation capability, deflection hardening tendency is still discernible in Fig. 3 at all ages. The use of artificial flaws yielded conflicting results, especially at the age of 6 hours. This might result from immature matrix fiber and flaw bonding that prevented the early-age HES-ECC mixtures from performing as a complete composite. Still, the rubber appears to perform better compared to expanded glass at this age. However, after 24 hours for both types of artificial flaws, the general trend was to improve the deflection capacity. Although the results did not indicate a predominance of a specific flaw type in improving the deflection value, at the end of 28 days it can be concluded that expanded glass stands out. It should be noted that expanded glass has a brittle nature compared to the ductile and soft rubber particles which have been shown to be effective on the flexural test results (Al-Fakih et al. 2021). It is also noteworthy that although the control mixtures produced with WPC exhibited a drastic decrease in deflection capacity compared to the calcium aluminate cement mixtures, both flaws worked effectively to raise the deflection capacity to a level comparable to the CAC mixtures. Increased deflection values and deflection-hardening behavior of HES-ECC mixtures with artificial flaws may also be attributed to the reduced first crack strength and increased margin for multiple cracking. Sample crack patterns associated with the artificial flaw types is given in Fig. 4.

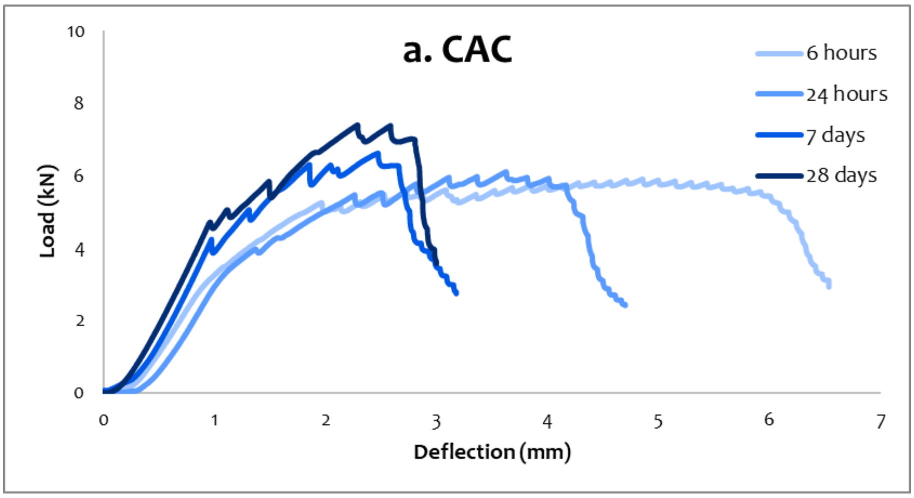


**Fig. 3.** (continued)

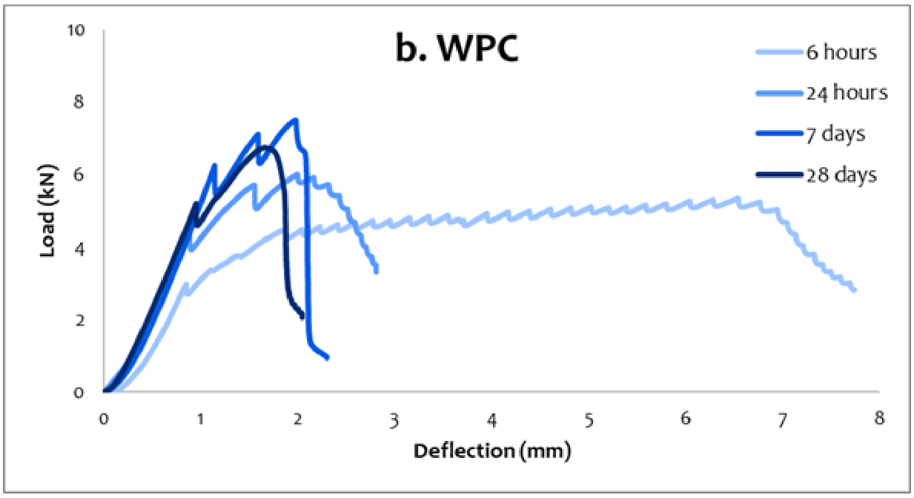


**Fig. 3.** Comparison of deflections at different ages for the control mixtures.

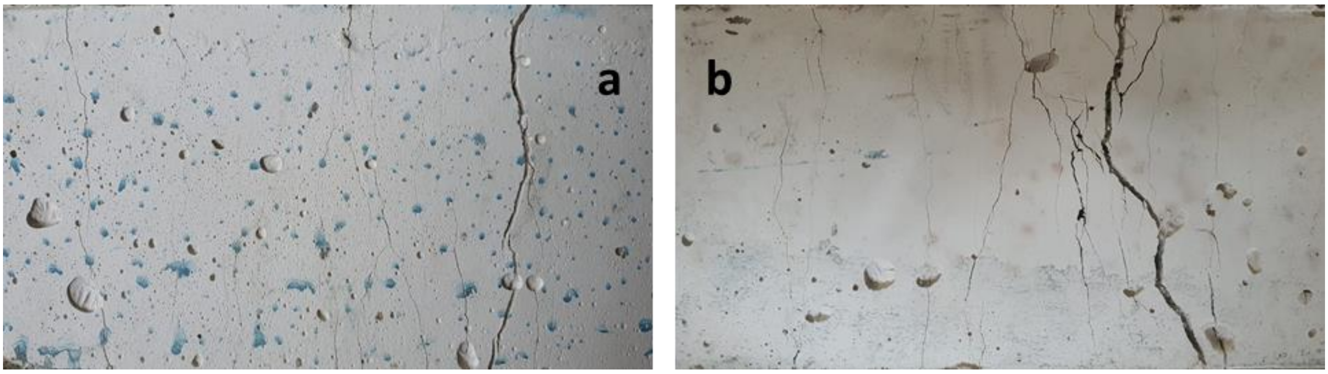


**Fig. 4.** Multiple cracking of expanded glass (a) and rubber (b) containing beams after failure.

### *3.3. Abrasion*

Abrasion resistance can be a critical property for high early-strength materials and the use of artificial flaws in such materials has the potential to substantially decrease their abrasion resistance. Fig. 5 shows the abrasion depth measured on the diameter of the area worn by rotating cutters for each testing age. It is immediately observable that all CAC and WPC mixtures exhibited an acceptable degree of abrasion resistance at all ages of testing. As the hydration reactions proceeded, the depths of abrasion clearly decreased. Nevertheless, the incorporation of both artificial flaws has a very narrow influence on abrasion resistance. The largest difference which is as low as around 0.05 mm, occurred at the age of 6 hours between the control mixture and the mixture containing rubber as an artificial flaw and may be attributed to pop up of the crumb rubber particles due to immature bond between the rubber and the matrix at this early stage of hydration. Besides, CAC mixtures showed a higher level of abrasion resistance at the early ages, however, the WPC mixtures performed better at the age of 28 days as they reached a higher degree of hydration. Keeping in mind that only 5% of flaws were used in the mixtures, it is difficult to make a comparison between the artificial flaws as the values were quite close but it can be concluded that expanded glass particles yielded a better abrasion resistance.

### *3.4. Drying shrinkage*

For a repair material, lack of dimensional compatibility with the repaired material is of significance as any restraining condition may result in cracking. In most cases, the repair materials are placed on a dimensionally stable existing material which makes the case more threatening. For high-performance materials like ECC, the degree of shrinkage is large due to the high amount of cementitious materials and very low w/c ratio which triggers the chemical shrinkage. Although the cracking resistors such as instantaneous and time-dependent tensile strain capacity of ECC can easily compensate for the shrinkage effect, yet it is important to have an idea of whether the artificial flaws drive the drying shrinkage for the sake of cracking potential. In Fig. 6, the drying shrinkage test results obtained from the length change measurements taken from bar specimens up to 90 days are provided. Drying shrinkage values vary depending on the duration of drying and the presence of artificial flaws in mixtures, as illustrated. The shrinkage values of all calcium aluminate cement mixtures increased remarkably up to 28 days, as expected, while the increase between 28 and 90 days was modest. On the other hand, results indicate that expanded glass and rubber particles have a minor impact on the shrinkage of calcium aluminate cement mixes. After 90 days, the drying shrinkage values for CAC mixtures varied in a short range between 1060 με and 1175 με.

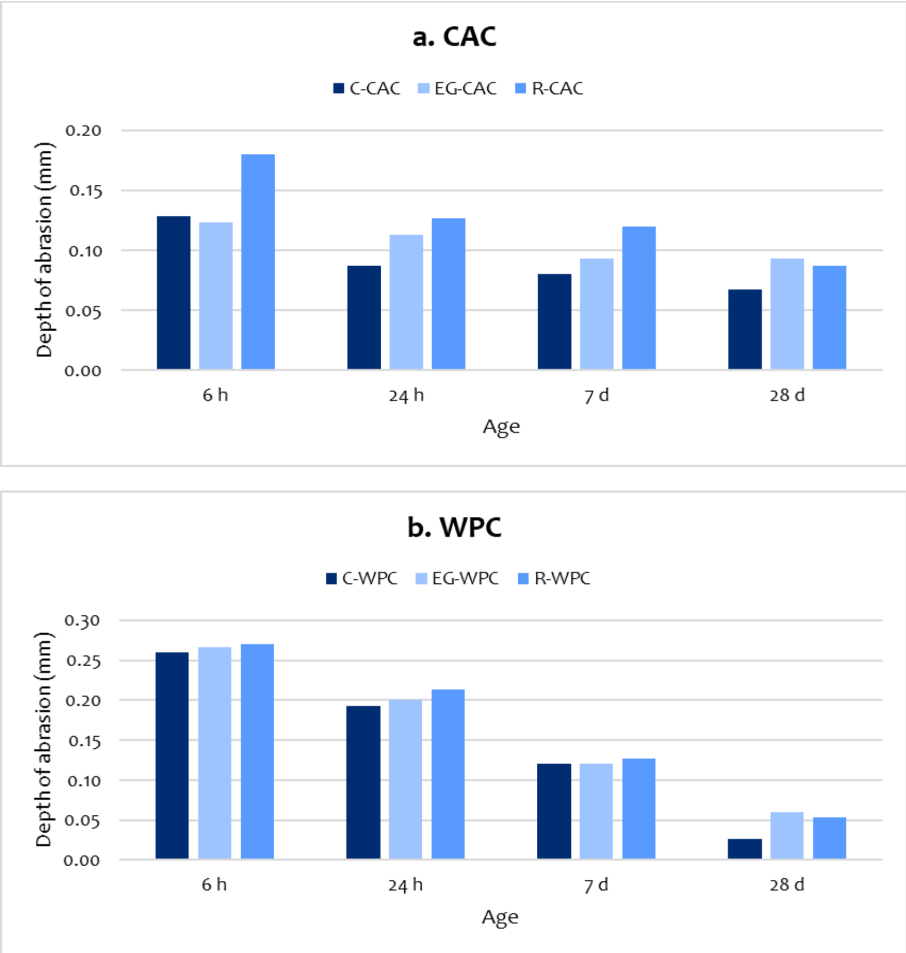


**Fig. 5.** Abrasion resistance of the mixtures.

Fig. 6 confirms that for all WPC mixtures, drying shrinkage values evolved significantly but not as sharply as for CAC mixtures until 28 days. The influence of artificial flaws on the drying shrinkage of WPC mixtures was more marked. The results revealed that when rubber particles are included in the mix, drying shrinkage rises. Incorporating expanded glass, on the other hand, resulted in the lowest drying shrinkage. The increase in the drying shrinkage in the case of crumb rubber usage as artificial flaws can be ascribed to the decrease of rigid particles to act as a restraint for shrinkage strains in the mixtures as described by Huang et al. (2013). The high absorption capacity of expanded glass may account for the reduction in drying shrinkage for mixtures containing expanded glass, as lightweight aggregates can absorb some of the mixing water and act as reservoirs that release the water during drying as mentioned by Ye et al. (2006) and Keskin et al. (2013).

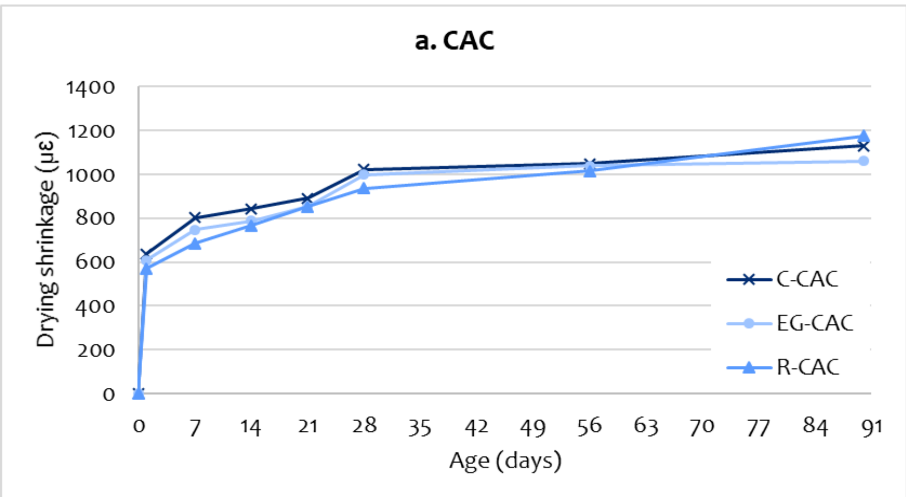


**Fig. 6.** (continued)

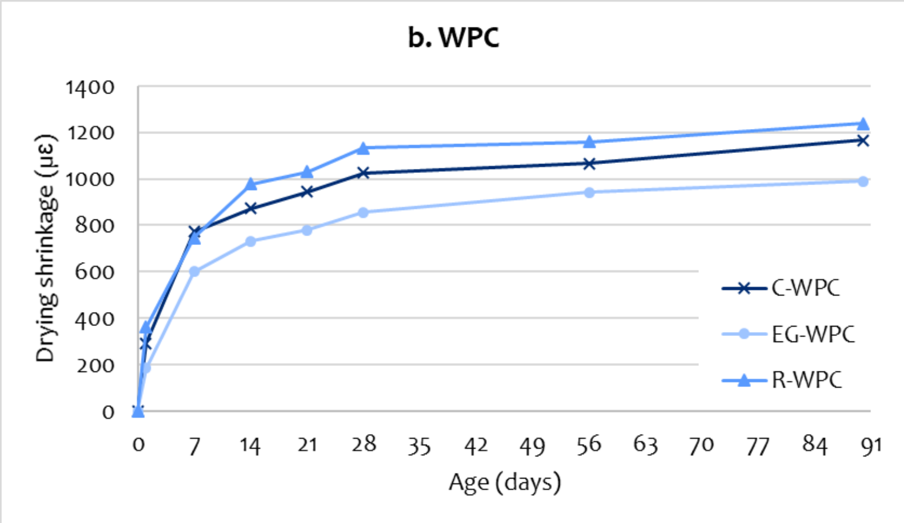


**Fig. 6.** Drying shrinkage of the mixtures.

### *3.5. Non-destructive tests*

Ultrasonic pulse velocity test was performed conforming to the ASTM C597 (2016) test method by using the indirect transmission method at predetermined testing ages and corresponding pulse velocities were calculated as presented in Table 6. Since UPV values are dependent on the elastic properties of the HES-ECC mixtures, they may serve to evaluate possible changes in the maturity hence the fracture toughness of the ECC mixtures as well. UPV values of all mixtures tested increased with time as hydration reactions progressed. For both of the cement types, the inclusion of artificial flaws resulted in a noticeable decrease in all UPV values, independent of the age of testing.

Nonetheless, UPV values were reduced the most by crumb rubber usage at all ages. This behavior was previously observed by other researchers (Albano et al. 2005; Marie 2016; Choi et al. 2022) as well and attributed to the decrease in the density and increase in the air content due to entrapped air on the rubber surface. Alongside the air entrainment, this reduction may also be ascribed to the damping effect of soft rubber particles.

**Table 6.** UPV values for HES-ECC prismatic specimens.

| Mixture ID | 6 hours (m/s) | 24 hours (m/s) | 7 days (m/s) | 28 days (m/s) |
|---|---|---|---|---|
| C-CAC | 4464 | 4626 | 4786 | 4931 |
| EG-CAC | 4406 | 4528 | 4717 | 4808 |
| R-CAC | 4293 | 4448 | 4609 | 4714 |
| C-WPC | 3963 | 4623 | 4874 | 5168 |
| EG-WPC | 3945 | 4508 | 4818 | 5072 |
| R-WPC | 3924 | 4369 | 4763 | 4992 |

The resonance frequency is an effective non-destructive test method mainly used for evaluating the concrete properties through the change in the dynamic modulus of elasticity. The test was performed in accordance with the ASTM C215 (1998) method. An accelerometer was employed to obtain the fundamental frequency of vibration for longitudinal and transversal modes after the beam specimen was struck with steel balls. By using the specimen size and mass along with the measured fundamental frequency, the related dynamic modulus of elasticity was calculated. Fig. 7 demonstrates the dynamic elastic modulus values calculated for transverse and longitudinal modes for CAC and WPC containing HES-ECCs. For both longitudinal and transversal modes, the values were close and all mixtures exhibited a similar ascending trend over time. CAC mixtures presented higher elastic modulus at 6 hours however the development of elastic modulus was greater for WPC mixtures. This tendency is also very similar to those observed in compressive and flexural strength test results which is predictable as strength and elastic modulus both increase as the degree of hydration increases. It is obvious that the flaws affect the test results in the same way regardless of the direction of testing. The incorporation of expanded glass contributed to a decrease of an average of 9% in dynamic elastic modulus after 28 days for mixtures with respect to control mixtures due to the weakness of expanded glass and the void content in expanded glass beads. Nevertheless, the lowest values were encountered in mixtures with crumb rubber particles with a decrease of an average of 13% which can be attributed to the high elasticity imparted by the resilient nature of the tire rubber. Moreover, in the case of CAC mixtures, the results obtained with both flaws were closer compared to the WPC mixtures where expanded glass mixtures are quite distinct with a higher elastic modulus which may be due to the bond characteristics of the flaws incorporated.

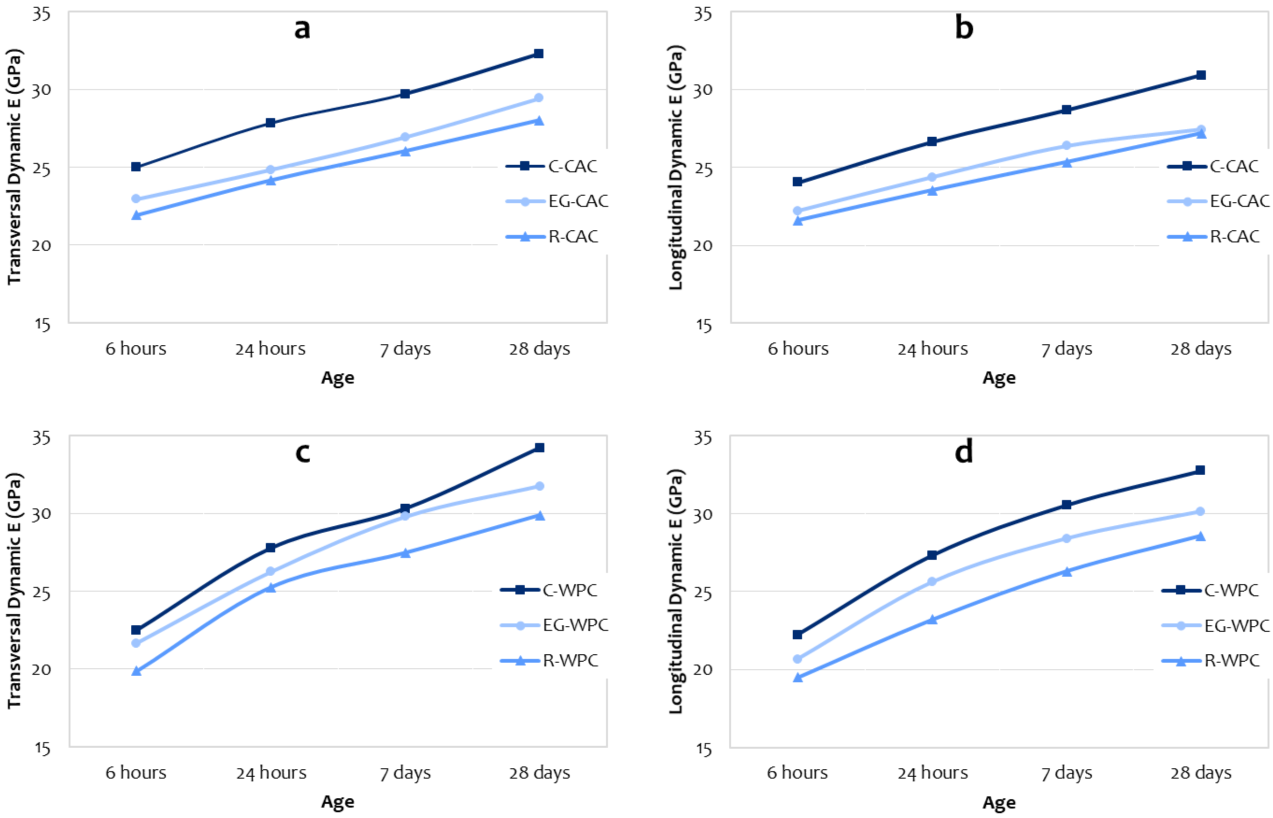


**Fig. 7.** Transversal (a, c) and longitudinal (b, d) dynamic *E* values for CAC (a, b) and WPC (c, d) mixtures.

The ability of cementitious materials to resist the electrical current is dependent on factors such as permeability, the presence of water in the pores, and the chemistry of the pore solution. As it depends on ion transfer through the specimen, a higher resistivity can infer better durability due to low permeability and a structure that is resistant to reinforcement bar corrosion. Thus, the electrical resistivity of the HES-ECC mixtures may indicate a potential durability issue driven by the presence of flaws and the high-strength binders.

As seen in Fig. 8, electrical resistivities of all mixtures were developed with time which can be attributed to a decrease in the size and quantity of water-filled capillaries as both the size and interconnectivity of the pores reduce as hydration products fill the pores and thus obstruct the electrical current. CAC mixtures were significantly more resistant to electric current than WPC mixtures, although the difference in strength values was not that substantial. In this case, it should also be noted that the electrical resistance also depends on the chemical composition of the pore solution and therefore does not necessarily give results in parallel with other test methods. Especially for CAC at early ages, high resistivity values were obtained ensuring a mixture with high resistivity to chloride penetration and a low possibility of reinforcement corrosion (Shane et al. 1999; ACI 2010). On the other hand, the resistance of WPC mixtures significantly increased continuously at all test ages. However, the development of resistivity was not rapid as CAC which gains most of its strength in a very short time after casting. For both cement types, the use of crumb rubber as an artificial flaw resulted in the highest resistivity which can be attributed to the dielectric nature of the rubber (Kaewunruen and Meesit 2016). Besides, expanded glass also enhanced the electrical resistivity of the mixtures as glass replacement is readily reported to improve the resistivity of cement-based materials in the previous studies (Her-Yung 2009; Kamali and Ghahremaninezhad 2015; Siad et al. 2017). It can be deduced that both of the flaws have potential positive effect on the corrosion protection of high early strength ECC mixtures.

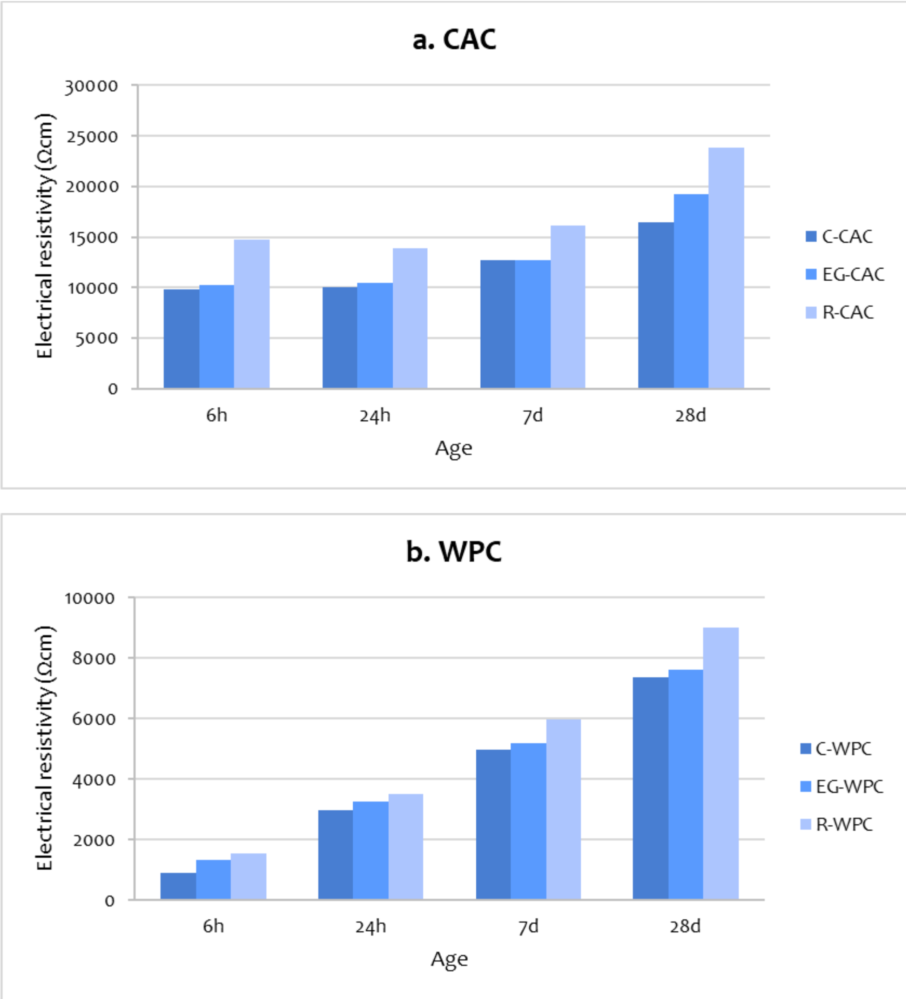


**Fig. 8.** Electrical resistivities of the mixtures.

## 4. Conclusions

This study evaluates the utilization of non-portland calcium aluminate cement as a primary binder for high-early strength Engineered Cementitious Composites design and compares it with conventionally used high early strength portland cement in terms of mechanical, abrasion, shrinkage and NDT properties while recycled materials of crumb rubber and expanded glass were employed as artificial flaws to ensure sufficient ductility. The results of the experimental study have led to the following conclusions:

It is possible to produce high early strength ECC mixtures by using both types of cement with a compressive strength well over 30 MPa at 6 hours after casting for the mixtures without any flaws. Calcium aluminate cement mixtures with lithium carbonate mixtures acquired this early strength without eliminating the entire amount of fly ash, while fly ash had to be removed in white portland cement mixtures.

For both cement types, most of the compressive strength was acquired before 24 hours, while the addition of 5% by volume artificial flaws reduced the compressive strength of both control mixtures to a limited extent. Crumb rubber addition resulted in a lower compressive strength compared to expanded glass, yet a satisfactory level of strength can be obtained for both of the flaw types.

Flexural strengths revealed a similar trend with the compressive strength as expected. While the deflection capacity of the control mixtures decreased with time, deflection hardening could be observed at all ages. Although flexural performances were similar for control mixtures at 6 hours, calcium aluminate cement mixtures exhibited higher deformability afterward. Both flaws significantly improved the deformation capacity of the HES-ECC mixtures.

All HES-ECC mixtures became more resistant to abrasion over time. Despite the increase in abrasion depths with the artificial flaws, their effect was minimal.

The drying shrinkages of calcium aluminate cement mixtures were not largely affected by the use of artificial flaws while for white portland cement mixtures, the effect of flaws was more pronounced. It is possible to conclude that the use of expanded glass reduces drying shrinkage for both cement types whereas the rubber particles resulted in an increase. In general, it can be claimed that the shrinkage values do not change in a way that critically increases the cracking potential.

As expected, the UPV and dynamic elastic modulus values increased with age and reduced when artificial flaws were added to the mixtures. Electrical resistivities were improved through the use of artificial flaws due to the low electrical conductivity of the artificial flaws used. Since rubber is a dielectric material, HES-ECC mixtures with rubber crumb exhibited the highest electrical resistance.

In light of all the mechanical, abrasion, shrinkage, and non-destructive testing results, it is evident that high early-strength ECC mixtures produced with calcium aluminate cement are suitable candidates for use in repair purposes. However, it is recommended to also consider the effects of potential effects of phase changes in the long term.

***Acknowledgements***

*Authors gratefully acknowledge Çimsa Mersin Cement Factory, Yatağan Thermal Power Plant, Polisan Construction Chemicals and BASF Chemical Company for their material support.*

***Funding***

*The authors received no financial support for the research, authorship, and/or publication of this manuscript.*

***Conflict of Interest***

*The authors declared no potential conflicts of interest with respect to the research, authorship, and/or publication of this manuscript.*

***Author Contributions***

*All of the authors made substantial contributions to conception and design, or acquisition of data, or analysis and interpretation of data; were involved in drafting the manuscript or revising it critically for important intellectual content; and gave final approval of the version to be published.*

***Data Availability***

*The datasets created and/or analyzed during the current study are not publicly available, but are available from the corresponding author upon reasonable request.*

## References

ACI (2010). ACI 222R-01 Protection of Metals in Concrete against Corrosion Reported by ACI Committee 222. ACI Committee Report. Farmington Hills, MI, USA.

Al-Fakih A, Mohammed BS, Liew MS (2021). On rubberized engineered cementitious composites (R-ECC): A review of the constituent material. *Case Studies in Construction Materials,* 14.

Albano C, Camacho N, Reyes J, Feliu JL, Hernández M (2005). Influence of scrap rubber addition to Portland I concrete composites: Destructive and non-destructive testing. *Composite Structures,* 71(3–4), 439–446.

ASTM C109 (2020). Standard Test Method for Compressive Strength of Hydraulic Cement Mortars (Using 2-in. or [50 mm] Cube Specimens). Annual Book of ASTM Standards (04 vol.). West Conshohocken, PA, USA.

ASTM C215 (1998). Standard test method for fundamental transverse, longitudinal, and torsional resonant frequencies of concrete specimens. Annual Book of ASTM Standards (4 vol.). West Conshohocken, PA, USA.

ASTM C494 (2013). Standard specification for chemical admixtures for concrete. Annual Book of ASTM Standards (04 vol.). West Conshohocken, PA, USA.

ASTM C596 (2007). Standard test method for drying shrinkage of mortar containing hydraulic cement. Annual Book of ASTM Standards (11 vol.). West Conshohocken, PA, USA.

ASTM C597 (2016). Standard test method for pulse velocity through concrete. American Society for Testing and Materials, West Conshohocken, PA, USA.

ASTM C944 (2007). Standard test method for abrasion resistance of concrete or mortar surfaces by the rotating-cutter method. Annual Book of ASTM Standards (99 vol.), West Conshohocken, PA, USA.

Choi Y, Kim IH, Lim HJ, Cho CG (2022). Investigation of strength properties for concrete containing fine-rubber particles using UPV. *Materials,* 15(10).

Emmons PH (1996). Concrete Repair and Maintenance Illustrated: Problem Analysis, Repair Strategy, and Techniques. R.S. Means, Wiley, New Jersey.

Emmons PH, Sordyl DJ (2006). The state of the concrete repair industry, and a vision for its future. *Concrete Repair Bulletin*, 7–14.

EN 14647 (2007). Calcium aluminate cement – Composition, specification and conformity criteria. British Standard (3 vol.).

FHWA (1998). Corrosion Protection: Concrete Bridges. Federal Highway Administration report FHWA-RD-98-088, Virginia, USA.

Frangopol DM, Furuta H (eds) (2001). Life-cycle cost analysis and design of civil infrastructure systems. Life-Cycle Cost Analysis and Design of Civil Infrastructure Systems. Reston, VA: American Society of Civil Engineers.

Her-Yung W (2009). A study of the engineering properties of waste LCD glass applied to controlled low strength materials concrete. *Construction and Building Materials,* 23(6), 2127–2131.

Ideker JH, Scrivener KL, Fryda H, Touzo B (2019). Calcium Aluminate Cements. *In: Hewlett PC, Liska M, editors, Lea's Chemistry of Cement and Concrete*, Butterworth-Heinemann, 537-584.

Huang X, Ranade R, Ni W, Li VC (2013). On the use of recycled tire rubber to develop low E-modulus ECC for durable concrete repairs. *Construction and Building Materials,* 46, 134–141.

Shane JD, Aldea CM, Bouxsein NF, Mason TO, Jenning HM, Shaw SP (1999). Microstructural and pore solution changes induced by rapid chloride permeability test measured by impedance spectroscopy. *Concrete Science and Engineering,* 1(2), 110–119.

Kaewunruen S, Meesit R (2016). Sensitivity of crumb rubber particle sizes on electrical resistance of rubberised concrete. *Cogent Engineering,* 3(1).

Kamali M, Ghahremaninezhad A (2015). Effect of glass powders on the mechanical and durability properties of cementitious materials. *Construction and Building Materials,* 98, 407–416.

Keskin SB, Sahmaran M, Yaman IO, Lachemi M (2014). Correlation between the viscoelastic properties and cracking potential of engineered cementitious composites. *Construction and Building Materials,* 71, 375–383.

Keskin SB, Sulaiman K, Sahmaran M, Yaman IO (2013). Effect of presoaked expanded perlite aggregate on the dimensional stability and mechanical properties of Engineered Cementitious Composites. *Journal of Materials in Civil Engineering,* 25(6), 763–771.

Kim YY, Kong HJ, Li VC (2003). Design of Engineered Cementitious Composite Suitable for Wet-Mixture Shotcreting. *ACI Materials Journal,* 100(6).

Kırca Ö (2006). Temperature Effect on Calcium Aluminate Cement Based Composite Binders. *Ph.D. Thesis,* Middle East Technical University, Ankara, Türkiye.

Kurtz S, Balaguru P, Condolazio G, Maher A (1997). Fast track concrete for construction repair. *Final Report*, Rutgers Department of Civil & Environmental Engineering, The State University, Piscataway, NJ.

Li M, Li VC (2011a). Cracking and healing of engineered cementitious composites under chloride environment. *ACI Materials Journal,* 108(3).

Li M, Li VC (2011b). High-early-strength engineered cementitious composites for fast, durable concrete repair-material properties. *ACI Materials Journal* 108(1), 3–12.

Li VC (1994). From micromechanics to structural engineering – the design of cementitious composites for civil engineering applications. *Structural Engineering/Earthquake Engineering,* 10(2).

Li VC (1997). Engineered cementitious composites (ECC) – tailored composites through micromechanical modeling. *Canadian Society for Civil Engineering*, 1–38.

Li VC (2003). On engineered cementitious composites (ECC). A review of the material and its applications. *Journal of Advanced Concrete Technology,* 1(3).

Li VC (2004). High performance fiber reinforced cementitious composites as durable material for concrete structure repair TT. *Restoration of Buildings and Monuments: an International Journal = Bauinstandsetzen und Baudenkmalpflege: eine Internationale Zeitschrift,* 10(2), 163–180.

Li VC (2012). Tailoring ECC for special attributes: A review. *International Journal of Concrete Structures and Materials* 6(3).

Li VC, Kanda T (1998). Innovations forum: Engineered Cementitious Composites for structural applications. *Journal of Materials in Civil Engineering,* 10(2), 66–69.

Li VC, Mishra DK, Naaman AE, Wight JK, LaFave JM, Wu HC, Inada Y (1994). On the shear behavior of engineered cementitious composites. *Advanced Cement Based Materials,* 1(3), 142–149.

Li VC, Wang S, Wu C (2001). Tensile strain-hardening behavior or polyvinyl alcohol engineered cementitious composite (PVA-ECC). *ACI Materials Journal,* 98(6), 483–492.

Lim YM, Li VC (1997). Durable repair of aged infrastructures using trapping mechanism of engineered cementitious composites. *Cement and Concrete Composites,* 19(4), 373–385.

Marie I (2016). Zones of weakness of rubberized concrete behavior using the UPV. *Journal of Cleaner Production,* 116, 217–222.

Parker F, Lee Shoemaker W (1991). PCC pavement patching materials and procedures. *Journal of Materials in Civil Engineering,* 3(1), 29–47.

Preetha R, Kumari K, Sakthi B, Harikumar CN, Abdul Gani HI (2023). Cause of distress of an old building through analytical and micro–analytical methods – a case study. *Challenge Journal of Concrete Research Letters*, 14(1), 18-30.

Qian S, Li VC (2007). Simplified inverse method for determining the tensile strain capacity of strain hardening cementitious composites. *Journal of Advanced Concrete Technology*, 5(2), 235–246.

Raupach M (2006). Concrete repair according to the new European Standard EN 1504. *Proceedings of the International Conference on Concrete Repair, Rehabilitation and Retrofitting*, ICCRRR 2005.

Şahmaran M, Li VC (2009). Durability properties of micro-cracked ECC containing high volumes fly ash. *Cement and Concrete Research* 39(11).

Şahmaran M, Li VC (2010). Engineered Cementitious Composites. *In Banthia N, Uomoto A, Bentur A, Shah S. P. (eds), Transportation Research Record: Journal of the Transportation Research Board (2164 vol.)*, 1–8. Vancouver: The University of British Columbia, Canada.

Şahmaran M, Al-Emam M, Yıldırım G, Şimşek YE, Erdem TK, Lachemi M (2015). High-early-strength ductile cementitious composites with characteristics of low early-age shrinkage for repair of infrastructures. *Materials and Structures/Materiaux et Constructions,* 48(5), 1389–1403.

Siad H, Lachemi M, Sahmaran M, Mesbah HA, Hossain KMA, Ozsunar A (2017). Potential for using recycled glass sand in engineered cementitious composites. *Magazine of Concrete Research,* 69(17), 905–918.

Soltan DG, Li VC (2018). A self-reinforced cementitious composite for building-scale 3D printing. *Cement and Concrete Composites,* 90, 1-13.

Spragg RP, Bu Y, Snyder KA, Bentz DP, Weiss J (2013). Electrical Testing of Cement-Based Materials: Role of Testing Techniques, Sample Conditioning, and Accelerated Curing. Joint Transportation Research Program.

Tarhan İH, Uysal H (2024). Strengthening of historic masonry vaults with CFRP prepreg. *Challenge Journal of Structural Mechanics*, 10(1), 1-6.

Wang S, Li VC (2006). High-early-strength engineered cementitious composites. *ACI Materials Journal,* 103(2), 97–105.

Whiting D, Nagi M (1994). Strength and durability of rapid highway repair concretes. *Concrete International,* 16(9), 36–41.

Wilson TP, Smith KL, Romine AR (1999). Materials and Procedures for Rapid Repair of Partial-depth Spalls in Concrete Pavements-Manual of Practice. *Federal Highway Administration*.

Woudhuysen J, Abley I (2004). Why is Construction so Backward? Willey Academy, Chichester, UK.

Yang E, Li VC 2007. Numerical study on steady-state cracking of composites. *Composites Science and Technology,* 67(2), 151–156.

Ye J, Hu S, Wang F, Zhou Y, Liu Z (2006). Effect of pre-wetted lightweight aggregate on internal relative humidity and autogenous shrinkage of concrete. *Journal Wuhan University of Technology, Materials Science Edition,* 21(1), 134–137.

Yildirim G, Şahmaran M, Al-Emam MKM, Hameed RKH, Al-Najjar Y, Lachemi M (2015). Effects of compressive strength, autogenous shrinkage, and testing methods on bond behavior of high-early-strength engineered cementitious composites. *ACI Materials Journal,* 112(3), 409–418.

Yokota H, Rokugo K, Sakata N (2008). Recommendations for design and construction of high performance fiber reinforced cement composites with multiple fine cracks. The Japan Society of Civil Engineers, Tokyo.

Yunovich M, Thompson NG (2003). Corrosion of highway bridges: economic impact and control methodologies. *Concrete International,* 25(1), 52–57.